BMC Neuroscience

RESEARCH Open Access

Ventromedial hypothalamic nucleus neuronal nitric oxide knockdown effects on GABAergic neuron metabolic sensor and transmitter marker gene expression in the male rat

Sagor C. Roy[1], Madhu Babu Pasula[1], Subash Sapkota[1] and Karen P. Briski[1,2*]

Abstract

The diffusible gas nitric oxide (NO) and amino acid γ-gamma-aminobutyric acid (GABA) exert contrary effects on glucose counterregulation in the male rat, but how these neurochemical signals integrate within ventromedial hypothalamic nucleus (VMN) neural circuitries remains unclear. Female rat dorsomedial (VMNdm) and ventrolateral (VMNvl) GABAergic neurons express neuronal nitric oxide synthase (nNOS) mRNA; notably these subpopulations exhibit dissimilar nNOS transcriptional responses to insulin-induced hypoglycemia (IIH). Here, nNOS gene knockdown tools were used to examine whether one or both VMN GABA neuron groups may be a target for nitrergic control of basal and hypoglycemic counterregulatory hormone secretion in the male. Data show that VMN nNOS gene knockdown respectively up- or down-regulated counterregulatory hormone profiles in eu- versus hypoglycemic male rats. Single-cell multiplex qPCR analysis of laser-catapult-microdissected GABA neurons showed that IIH elevated nNOS gene expression in GABA neurons from each VMN division, yet nNOS siRNA pretreatment attenuated distinctive IIH-associated transmitter marker gene expression patterns in VMNdm versus VMNvl GABAergic neurons. nNOS gene silencing had similar effects on glucokinase and glucose transporter gene responses to IIH in each GABA neuron subpopulation but elicited division-specific effects on mRNA encoding 5-AMP-activated protein kinase (AMPK) alpha/catalytic subunits and the lactate membrane receptor GPR81/HCAR1. Current findings provide original evidence that VMN NO may impose bi-directional, glucose status-contingent control of counterregulatory hormone outflow in the male rat. Data moreover imply that during IIH, NO may control distinctive sources of metabolic sensory regulatory stimuli in VMNdm versus VMNvl GABA neurons and may shape unique counterregulation-controlling neurochemical transmission by each cell population.

Keywords nNOS siRNA, GABA neuron, GAD1/2, Glucokinase, AMPK, Glucagon

*Correspondence:
Karen P. Briski
briski@ulm.edu
[1]School of Basic Pharmaceutical and Toxicological Sciences, College of Pharmacy, University of Louisiana Monroe, Monroe, LA 71201, USA
[2]UL System Foundation and Willis-Knighton Health Systems Professorship in Toxicology, College of Pharmacy, University of Louisiana at Monroe, Rm 356 Bienville Building, 1800 Bienville Drive, Monroe, LA 71201, USA

Introduction

Glucose is utilized at a disproportionately high rate by the brain to maintain critical high energy-requiring nerve cell functions. Hypoglycemia-associated disruption of those functions can lead to neurological impairment and injury/destruction of vulnerable neuron populations [1–3]. Systemic glucose homeostasis is maintained by an expansive neural network that extends throughout the central neuroaxis, encompassing several major brain regions including the diencephalic hypothalamus [4]. Neurons that operate in this dedicated circuitry perform various distinctive functions including acquisition of metabolic sensory cues, integration of convergent regulatory signals, or efferent innervation of peripheral effectors. Neurotransmitters that impact neural regulation of body-wide glucostasis have been identified, yet comprehension of the linear organization and functional interconnectivity of nerve cells that comprise this network and knowledge of how those nerve cell units may respond to modulatory metabolic, endocrine, and neurochemical stimuli to affect overall system operation remains elusive.

The hypothalamus operates as the hierarchal autonomic motor center in the brain, imposing final, coordinated control of autonomic, neuroendocrine, and behavioral functions that rectify glucose imbalance. Neurons in the ventromedial hypothalamic nucleus (VMN), a prominent bilateral component of the mediobasal hypothalamus (MBH), express gene transcripts that encode protein markers for neurochemicals that regulate hypoglycemic patterns of glucagon and corticosterone secretion, namely the amino acid transmitters γ-aminobutyric acid (GABA) and glutamate; the labile lipid-permeable gas nitric oxide (NO); and the neuropeptide growth hormone-releasing hormone (Ghrh) [5–7]. There is a critical need to characterize the local (i.e., intra-VMN) and extra-VMN cellular targets of these neurotransmitter signals. In the VMN, the possibility that these distinctive counterregulatory stimuli may be integrated within a common circuitry has not been explored. While a plausible, conventional assumption is that these neurochemicals may converge, directly and/or indirectly, upon one or more shared VMN substrates, an alternative prospect is that these signals may operate within an ordered, organized cascade. As NO acts over an extremely limited diffusion range after nitric oxide synthase (NOS)-catalyzed generation from L-arginine [8], it is a logical candidate for potential local modulatory manipulation of VMN counterregulatory neurotransmission. Recent studies show that female rat VMN GABAergic neurons express mRNA for the nerve cell-specific NOS enzyme isoform neuronal NOS (nNOS), and that GABA nerve cell subpopulations located in dorsomedial (VMNdm) versus ventrolateral (VMNvl) divisions of the VMN exhibit disparate nNOS transcriptional reactivity to insulin-induced hypoglycemia (IIH) [7]. Studies in the male were the first to document NO involvement in glucose counterregulation, reporting that this neurochemical acts on as-yet-unidentified MBH targets to maximize IIH-induced counterregulatory hormone secretion in that sex [9, 10]. Current studies used in vivo gene silencing tools and a validated whole-animal model for IIH to investigate the foundational hypothesis that NO may act on targets within in the VMN to regulate basal and/or hypoglycemic counterregulatory hormone secretion patterns. To address the correlated premise that NO may control VMNdm and/or VMNvl GABAergic neuron input to local counterregulatory neural networks, a combinative approach involving in situ immunocytochemical identification of individual VMN glutamate decarboxylase$_{65/67}$ (GAD$_{65/67}$)- immunoreactive neurons for sequential laser-catapult microdissection and single-cell multiplex qPCR methods was used to examine if and how VMN nNOS gene silencing may affect expression of genes that encode protein markers for GABA and characterized co-expressed counterregulatory neurochemicals in each VMN GABAergic nerve cell group.

Specialized sensors located in discrete central and peripheral structures supply dynamic sensory feedback on cellular glucose and energy stability to the brain glucostatic network [11]. Multiple glucose sensing mechanisms operate in the brain, including screening by glucose transporter2 (GLUT2) at the critical juncture of plasma membrane uptake and by the specialized hexokinase glucokinase (GCK) at the initial rate-limiting step of glycolysis, which involves transfer of phosphate from ATP to glucose to generate glucose-6-phosphate [12–16]. Brain cell ATP depletion is communicated by the ultrasensitive energy sensor 5'-AMP-activated protein kinase (AMPK), which is activated by phosphorylation of the threonine reside 172 in response to decrements in the AMP/ATP ratio [17, 18]. AMPK restores cellular energy balance by activating processes that generate energy, i.e. lipid oxidation, glucose uptake, while inhibiting those that consume energy, e.g. protein synthesis. AMPK is a heterotrimeric complex composed of catalytic (alpha) and regulatory (beta, gamma) subunits. Protein kinase AMP-activated catalytic subunits alpha 1 (AMPKα1) and alpha (AMPK α2) are activated to a similar extent in response to increased intracellular AMP but exhibit dissimilar substrate specificity which may impose divergent effects on cell function [19]. There is compelling evidence that hypothalamic GCK and AMPK provide critical input to neural pathways that regulate body-wide energy and glucose stability. VMN neurons have the evident capacity to gauge and signal reductions in cellular energy status as subsets of these nerve cells exhibit augmentation or diminution of synaptic firing rates in response to declining ambient energy substrate levels. VMN GABAergic

neurons are apparently a source of metabolic sensory cues as these cells express gene transcripts for GCK and AMPKα1 and -α2 [20]. Notably, IIH causes dissimilar adjustments in these sensor gene profiles in VMNdm versus VMNvl GABA nerve cells in the female rat. Present studies leveraged multiplex qPCR analytical techniques to address the question that VMN NO may regulate basal and/or hypoglycemic patterns of GLUT2, GCK, and/or AMPK catalytic subunit isoform gene expression in GABAergic neurons residing in the male rat VMNdm and/or VMNvl.

Brain astrocytes are a vital contributor to neuronal metabolic stability as these neuroglia take up glucose from the circulation, amass this energy substrate in the form of the complex polysaccharide glycogen, and convert glucose to the trafficable oxidizable metabolic fuel L-lactate. Recent studies affirm that VMN counterregulatory, including GABA, neurotransmission is shaped by lactate signaling [21, 22]. Lactate apparently acts, in part, as a volume transmitter to shape VMNvl GABA release as this nerve cell subpopulation expresses the G protein-coupled plasma membrane lactate receptor GPR81/hydroxycarboxylic acid receptor-1 (HCAR1), and VMN GPR81 gene knockdown alters counterregulatory hormone outflow and VMNvl GABA neuron $GAD_{65/67}$ protein profiles [23]. It was of interest here to investigate whether GPR81 mRNA is expressed in both VMNdm and VMNvl GABA neurons, and to determine if and how VMN nNOS gene knockdown may affect this important gene profile in one or both subpopulations.

Materials and methods

Animals

Adult male Sprague Dawley adult rats (300–400 gm *bw*; Envigo RMS, Inc., Indianapolis, ID) were housed in groups of 2–3 animals per cage, under a 14 h light/10 h dark cycle (lights on at 05.00 h). Animals had unrestricted access to standard laboratory chow (Harlan Teklad LM-485; Harlan Industries, Madison, WI) and water, and were acclimated to daily handling before experimentation was initiated. Study protocols and procedures were carried out in accord with the NIH Guide for Care and Use of Laboratory Animals, 8th Edition, with ULM Institutional Animal Care and Use Committee approval. All studies were performed in conformance with ARRIVE guidelines.

Experimental design

Animals were randomly assigned to one of four treatment groups ($n = 6$/group). On day 1, rats were anesthetized by intraperitoneal injection of ketamine/xylazine (0.1 mL/100 g *bw*; 90 mg ketamine:10 mg xylazine/mL; Henry Schein Animal Health, Dublin, OH) prior to bilateral intra-VMN infusion of Scramble siRNA (SCR; groups 1 and 3; Accell™ Control Pool Non-Targeting, 500 pmol; prod. no. D-001910-10-20; Horizon Discovery, Waterbeach, UK Dharmacon™, UK) or nNOS siRNA (groups 2 and 4; Accell™ Rat nNOS/NOS1 siRNA, set of 4 (target sequences: CUAUCGGCUUUAAGAAAUU; CCCUC UAGCCAAAGAAUUU; GUCACAGGUCUGGGUAA UG; UCCUUAACA-ACCCGUAUUC; 500 pmol; prod. no. A-100575-16-0010; Horizon Disc.) in a total 1.0 µL volume, at an infusion rate of 3.6 µL/min, to pre-determined three-dimensional coordinates [2.5 mm posterior to *bregma*; 0.6 mm lateral to midline; 9.0 mm ventral to skull surface], using described methods [5–7]. Infusions were performed using a 33-gauge Neuros syringe (prod. no. 53496; Stoelting Co., Wood Dale, IL), aided by a Neurostar stereotactic Drill and Injection Robot (Neurostar, Tubingen, Germany), featuring automated drilling, atlas-integrated intuitive computerized stereotaxic frame control, including *bregma* setting and alignment correction, and dynamic computerized image-based monitoring of needle placement. Post-surgical treatments included ketoprofen (1 mg/ml/kg *bw sc*; Bayer Health Care LLC, Animal Health Division, S. Mission, Kansas) and enrofloxacin (10 mg/0.1 mL IM; Bayer Health) injections and topical application of 0.25% bupivacaine (Hospira Inc., IL) to closed incisions. Animals were transferred to individual cages after full post-operative recovery. At 09:00 h on day 7, animals were injected *sc* with vehicle (V; sterile insulin diluent; Eli Lilly & Company, Indianapolis, IN; groups 1 and 2;) or neutral protamine Hagedorn (NPH) insulin (INS; 10 U/kg *bw* [24]; Eli Lilly; groups 3 and 4). Unanesthetized animals were sacrificed at 10:00 h by rapid decapitation in a rodent guillotine for brain and trunk blood collection. Dissected whole brains were snap-frozen in dry ice-cooled isopentane for storage at -80 °C. Plasma was stored at -20 °C.

Single-cell VMNdm and VMNvl GABAergic neuron laser-catapult-microdissection

Consecutive 10 µm-thick frozen sections were cut through the VMN of each brain between – 1.8 mm to -2.3 mm posterior to *bregma* and mounted on polyethylene naphthalate membrane-coated slides (prod. no. 415190-9041-000; Carl Zeiss Microscopy LLC, White Plains, NY) for immunocytochemical processing and laser-catapult-microdissection. In situ immunolabeling of VMN GABA neurons was performed as reported [25–28]. Individual VMNdm and VMNvl $GAD_{65/67}$–ir neurons were removed from tissue sections using a Zeiss P.A.L.M. UV-A microlaser IV (Carl Zeiss), using described methods [25–28; Supplementary Fig. 1], and collected into separate adhesive caps (prod. no. 415190-9181-000; Carl Zeiss) containing SingleShot™ Cell Lysis kit buffer supplemented with SingleShot™ DNase and SingleShot™ Proteinase K (4.0 uL; prod. no. 1725080;

Bio-Rad Laboratories, Hercules, CA). For each animal, $n = 2$ VMNdm and $n = 2$ VMNvl GABAergic neurons were acquired for single-cell gene expression analysis.

Single-cell multiplex reverse transcription quantitative polymerase chain reaction (RT-qPCR) analysis

Complementary DNA (cDNA) Synthesis and Amplification: Individual cell lysates were obtained by centrifugation *(*3000 rpm; 4℃), then incubated at 25 °C (10 min) and at 75 °C (5 min) in *an* iQ5 iCycler (Bio-Rad, Hercules, CA) to remove genomic DNA. Lysate RNA quantity and purity were verified by NanoDrop spectrophotometry (prod. no. ND-ONE-W, ThermoFisherScientific, Waltham, MA). RNA samples were reverse-transcribed to cDNA by addition of iScript™ Advanced cDNA Synthesis kit reagents (prod. no. 1725038; Bio-Rad) and centrifugation at 46 °C (20 min) and 95 °C (1 min), as reported [29–31]. A preamplification master mix was prepared by combining a pool of 15 PrimePCR™ PreAmps for SYBR® Green Assays [GAD1/GAD67 (prod. no. qRnoCID0004554), GAD2/GAD65 (prod. no. qRnoCID0003485), nNOS/NOS1 (prod. no. qRnoCED0009301), Ghrh (prod. no. qRnoCID0007723), SF-1/Nr5a1 (prod. no. qRnoCID0001458), GPR81/HCAR1 (prod. no. qRnoCED0001040), GCK (prod. no. qRnoCID0009394), AMPKα1/PRKAA1 (prod. no. qRnoCID0001262), AMPKα1/PRKAA2 (prod. no. qRnoCID0006799), excitatory amino acid transporter-2 (EAAT-2/Slc1A2) (prod. no. qRnoCED0005967), GLUT2/Slc2A2 (prod. no. qRnoCID0009479), GLUT3/Slc2A3 (prod. no. qRnoCID0004167), housekeeping gene glyceraldehyde-3-phosphate dehydrogenase (GAPDH) (prod. no. qRnoCID0057018)] with SsoAdvanced™ PreAmp Supermix (prod. no. 1725160; Bio-Rad). Supplementary Table 1 contains information on individual PrimePCR™ target gene assays performed here. After addition of pre-amplification master mix (9.5 µL), individual cDNA samples were incubated at 95 °C (3 min) followed by 22 cycles of (1) 95 °C (15 s), followed by (2) 60 °C (4 min). *RT-qPCR Analysis*: Pre-amplified cDNA samples were diluted with IDTE (prod. No. 11-05-01-05; 1X TE solution; Integrated DNA Technologies, Inc., Coralville, IA). Aliquots of diluted sample (2.0 µL) were combined with Bio-Rad target gene primers [GAD1/GAD67 (0.5 µL; prod. no. qRnoCID0004554), GAD2/GAD65 (0.5 µL; prod. no. qRnoCID0003485), nNOS/NOS1 (0.5 µL; prod. No. qRnoCED0009301), Ghrh (0.5 µL; prod. no. qRnoCID0007723), SF-1/Nr5a1 (0.5 µL; prod. no. qRnoCID0001458), GCK (0.5 µL; prod. no. qRnoCID0009394), GPR81/HCAR1 (0.5 µL; prod. no. qRnoCED0001040), GLT-1/Slc1A2 (0.5 µL; prod. no. qRnoCED0005967), GLUT2/Slc2A2 (0.5 µL; prod. no. qRnoCID0009479), GLUT3/Slc2A3 (0.5 µL; prod. no. qRnoCID0004167), AMPKα1/PRKAA1 (0.5 µL; prod. no. qRnoCID0001262), AMPKα2/PRKAA2 (0.5 µL; prod. no. qRnoCID0006799), GAPDH (0.5 µL; prod. no. qRnoCID0057018)], and iTaq™ Universal SYBR® Green Supermix (5.0 µL; prod. no, 1725121, Bio-Rad), as reported [5–7, 20]. Samples were analyzed in PCR plate wells (prod. no. HSP3805, Bio-Rad) in a Bio-Rad CFX384™ Touch Real-Time PCR Detection System, under the following conditions: initial denaturation at 95 °C (30 s), followed by 40 cycles of (1) 95 °C incubation (3 s) and (2) 45 s incubation at 57.3 °C for GLUT3, 60.5 °C for PRKAA1 and PRKAA2, 60 °C for GAD1/GAD_{67}, GAD2/GAD_{65}, and GPR81, 59.1 °C for SF-1/Nr5a1, 59.5 °C for GCK, 58.0 °C for Ghrh and NOS1/nNOS, 57.3 °C for GLT-1/Slc1A2, Slc2A2, Slc2A3, and GAPDH. CT limit of amplification was set at 35. Melt curve analyses were carried out to identify nonspecific products and primer dimers. Gene expression data were normalized to the housekeeping gene GAPDH by the $2^{-\Delta\Delta Ct}$ or comparative Ct method [32].

Glucose and counterregulatory hormone measurements

Plasma glucose levels were measured in duplicate using an ACCU-CHECK Aviva plus glucometer per manufacturer's recommendations (Roche Diagnostic Corporation, Indianapolis, IN) [24]. Circulating corticosterone and glucagon concentrations were analyzed in duplicate with commercial kit reagents (Corticosterone ELISA kit, prod. no. ADI-900-097; Enzo Life Sciences, Inc., Farmingdale, NY; Glucagon ELISA kit, prod. no. EZGLU-30 K, EMD Millipore, Billerica, MA) [5].

Statistics

Mean normalized VMNdm or VMNvl mRNA, glucose, and counterregulatory hormone values were analyzed between treatment groups by two-way analysis of variance and Student Newman Keuls *post-hoc* test using IBM SPSS 22.0 software. Differences of $p < 0.05$ were considered significant. In each figure, statistical differences between specific pairs of treatment groups are denoted as follows: $^{*}p < 0.05$; $^{**}p < 0.01$; $^{***}p < 0.001$; $^{****}p < 0.0001$.

Results

NO acts on as-yet-unknown targets in the male rat MBH to shape glucose counterregulation. Current studies involved site-targeted SCR versus nNOS siRNA administration to determine if VMN NO controls eu- and/or hypoglycemic patterns of counterregulatory hormone release in this sex. VMN GABAergic neurons in the female rat express nNOS mRNA but exhibit neuroanatomical division, i.e. VMNdm- versus VMNvl-specific adjustments in nNOS gene expression during IIH [Roy et al., 2024]. Here, complimentary in situ immunocytochemistry/laser-catapult microdissection/single-cell multiplex qPCR techniques were used to investigate VMN GABA nerve cell metabolic sensor and counterregulatory

neurochemical marker gene transcriptional reactivity to VMN nNOS gene silencing in eu- and hypoglycemic male rats.

Effects of intra-VMN nNOS siRNA administration on eu- and hypoglycemic patterns of nNOS gene expression in VMN GABAergic neurons are shown in Fig. 1. Data document the efficacy of this gene silencing paradigm for down-regulation of nNOS mRNA in VMNdm [Fig. 1A; SCR siRNA/*sc* V (blue box-and-whisker plot; $n=12$) versus nNOS siRNA/*sc* V (yellow box-and-whisker plot; $n=12$); $F_{(3,44)}$: 119.29, $p<0.001$; Knockdown main effect: $F_{(1,44)}$: 232.90, $p<0.001$; INS main effect: $F_{(1,44)}$: 9.80, $p=0.003$; Knockdown/INS interaction: $F_{(1,44)}$: 115.16, $p<0.001$] and VMNvl [Fig. 1B; $F_{(3,44)}$: 752.57, $p<0.001$; Knockdown main effect: $F_{(1,44)}$: 584.57, $p<0.001$; INS main effect: $F_{(1,44)}$: 1654.27, $p<0.001$; Knockdown/INS interaction: $F_{(1,44)}$: 18.86, $p<0.001$] GABAergic neurons. Data show that IIH [SCR siRNA/*sc* INS (green box-and-whisker plot; $n=12$) versus SCR siRNA/*sc* V] amplified nNOS gene transcription in each GABA nerve cell subpopulation and that this stimulatory response was attenuated by nNOS siRNA pretreatment [nNOS siRNA/*sc* INS (orange box-and-whisker plot; $n=12$) versus SCR siRNA/*sc* INS].

Data in Fig. 2 illustrate effects of VMN nNOS gene knockdown on GAD1/GAD_{67} and GAD2/GAD_{65} gene profiles in VMNdm (Fig. 2A and C) versus VMNvl (Fig. 2B and D) $GAD_{65/67}$-ir neurons collected from V- or INS-injected male rats. Data indicate that nNOS siRNA decreased baseline GAD1 mRNA levels in VMNdm [Fig. 2A; $F_{(3,44)}$: 23.33, $p<0.001$; Knockdown main effect: $F_{(1,44)}$: 0.18, $p=0.671$; INS main effect: $F_{(1,44)}$: 1.27, $p=0.266$; Knockdown/INS interaction: $F_{(1,44)}$: 68.53, $p<0.001$] and VMNvl [Fig. 2B; $F_{(3,44)}$: 213.56, $p<0.001$; Knockdown main effect: $F_{(1,44)}$: 202.79, $p<0.001$; INS main effect: $F_{(1,44)}$: 177.08, $p<0.001$; Knockdown/INS interaction: $F_{(1,44)}$: 260.81, $p<0.001$] GABA neurons. IIH decreased this gene profile in both GABA neuron subpopulations. This inhibitory response was averted by nNOS siRNA pretreatment in VMNdm GABA nerve cells but was exacerbated by nNOS gene silencing in the VMNvl cell group. As shown in Fig. 2C, baseline VMNdm GABA neuron GAD2 gene transcription was suppressed by nNOS gene knockdown [$F_{(3,44)}$: 57.42, $p<0.001$; Knockdown main effect: $F_{(1,44)}$: 82.09, $p<0.001$; INS main effect: $F_{(1,44)}$: 79.20, $p<0.001$; Knockdown/INS interaction: $F_{(1,44)}$: 10.98, $p=0.002$]. Hypoglycemic down-regulation of this mRNA was unaffected by nNOS siRNA. Data presented in Fig. 2D disclose that VMN nNOS gene knockdown down-regulated VMNvl GABA neuron GAD2 gene transcription in V- and INS-injected animals [$F_{(3,44)}$: 499.30, $p<0.001$; Knockdown main effect:

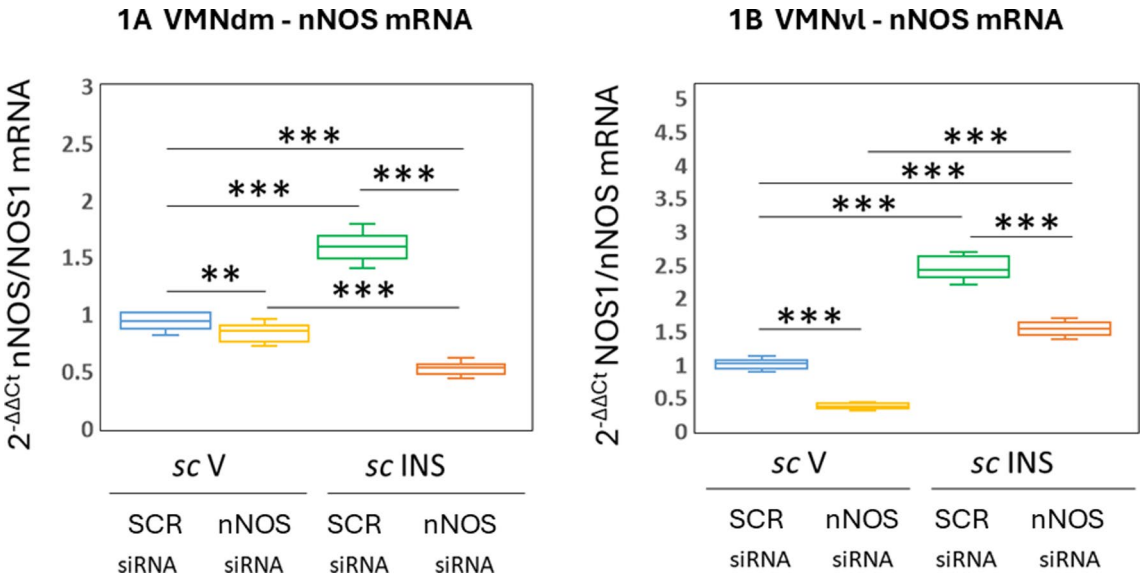

Fig. 1 Effects of Ventromedial Hypothalamic Nucleus (VMN) Neuronal Nitric Oxide Synthase (nNOS) Gene Silencing on Dorsomedial VMN (VMNdm) or Ventrolateral VMN (VMNvl) γ-Aminobutyric Acid (GABA) Neuron nNOS Gene Expression in the Male Rat. Groups of adult male rats ($n=6$/group) were pretreated by bilateral stereotactic administration of control/scramble (SCR) or nNOS siRNA to the VMN, then injected subcutaneously (*sc*) with vehicle (V) or neutral protamine Hagedorn insulin (INS; 10.0 U/kg *bw*) one hour before sacrifice. Individual VMNdm and VMNvl GABAergic neurons were labeled in situ by immunocytochemical methods for GAD65/67-immunoreactivity (-ir) prior to laser-catapult-microdissection for single-cell multiplex qPCR analysis. mRNA data were normalized to the housekeeping gene GAPDH by the $2^{-\Delta\Delta Ct}$ method. Gene expression data are presented here in box-and-whisker plot format, which displays the median, lower and upper quartiles, and lower and upper extremes of a data set. Plots depict normalized nNOS values for VMNdm (Fig. 1**A**) and VMNvl Fig. 1**B**) GABAergic neurons collected from the following treatment groups: SCR siRNA/*sc* V (blue box-and-whisker plots, $n=12$), nNOS siRNA/*sc* V (yellow box-and-whisker plots; $n=12$), SCR siRNA/ *sc* INS (green box-and-whisker plots; $n=12$), nNOS siRNA/*sc* INS (orange box-and-whisker plots; $n=12$). Statistical differences between discrete pairs of treatment groups are denoted as follows: *$p<0.05$; **$p<0.01$; ***$p<0.001$

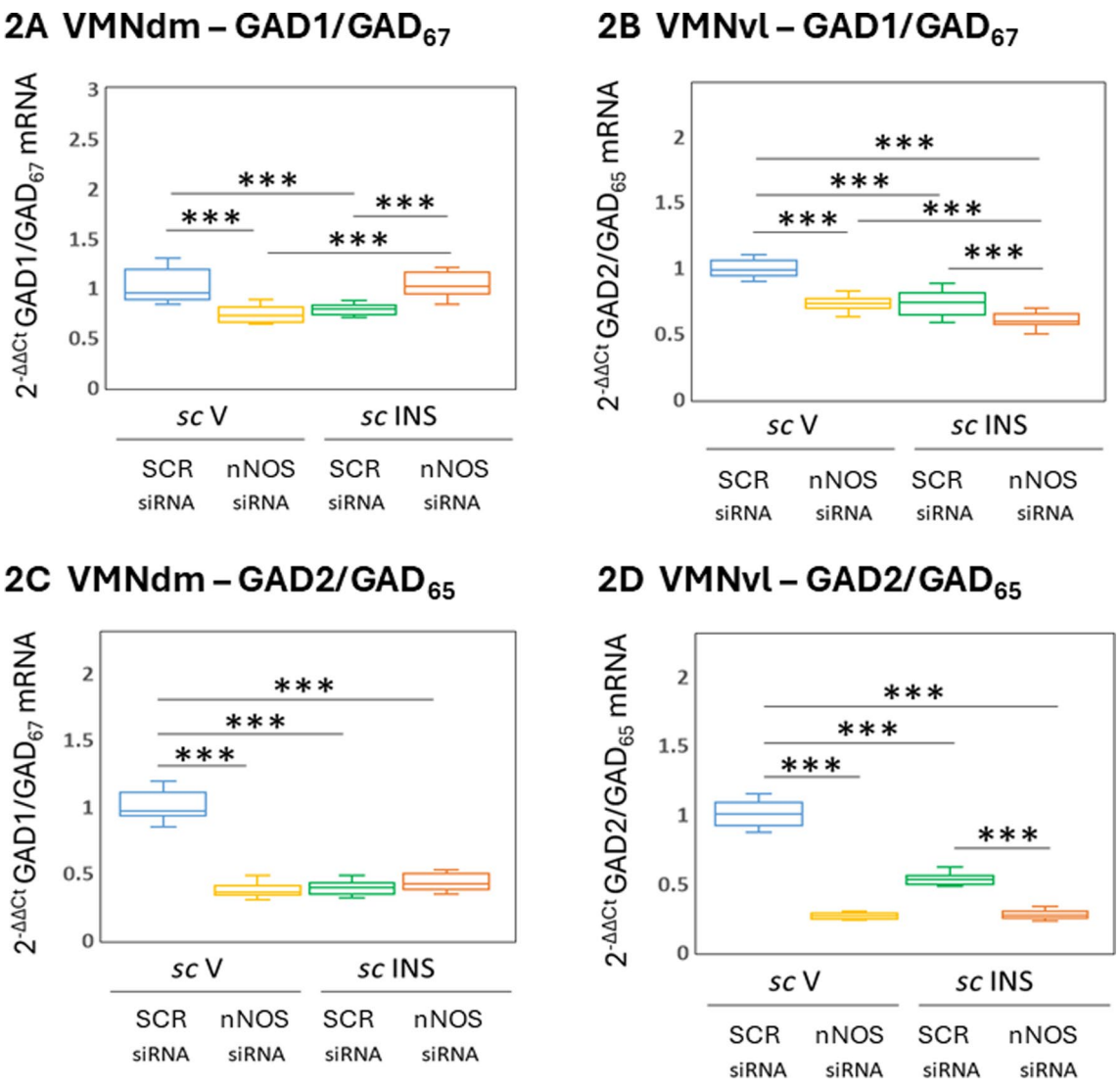

Fig. 2 Effects of VMN nNOS siRNA Administration on VMNdm versus VMNvl γ-Aminobutyric Acid (GABA) Neuron Glutamate Decarboxylase-1 (GAD1/GAD67) and – 2 (GAD2/GAD_{65}) Gene Expression in the Male Rat. Male rats randomly assigned to one of four experimental groups were pretreated by bilateral intra-VMN SCR or nNOS siRNA infusion prior to *sc* V or INS injection. Individual laser-catapult-microdissected $GAD_{65/67}$-ir neurons from the VMNdm or VMNvl were analyzed for multiplex gene expression. mRNA data were normalized to the housekeeping gene GAPDH using the $2^{-\Delta\Delta Ct}$ method. The box-and-whisker plot format used here depicts median, lower and upper quartiles, and lower and upper extremes of a data set. Plots depict normalized $GAD1/GAD_{67}$ [Fig. 2**A** (VMNdm) and 2**B** (VMNvl)] or $GAD2/GAD_{65}$ [Fig. 1**C** (VMNdm) and 1**D** (VMNvl)] mRNA values for GABA neurons collected from subjects in the following treatment groups: SCR siRNA/*sc* V (blue box-and-whisker plots, $n = 12$), nNOS siRNA/*sc* V (yellow box-and-whisker plots; $n = 12$), SCR siRNA/ *sc* INS (green box-and-whisker plots; $n = 12$), nNOS siRNA/*sc* INS (orange box-and-whisker plots; $n = 12$). Statistical differences between discrete pairs of treatment groups are denoted as follows: $^{*}p < 0.05$; $^{**}p < 0.01$; $^{***}p < 0.001$

$F_{(1,44)}$: 1033.69, $p < 0.001$; INS main effect: $F_{(1,44)}$: 233.00, $p < 0.001$; Knockdown/INS interaction: $F_{(1,44)}$: 241.23, $p < 0.001$].

Figure 3 illustrates effects of VMN nNOS gene silencing on GABAergic nerve expression of mRNAs that encode the counterregulation-enhancing neuropeptide Ghrh (Fig. 3A and B) and Slc1A2, transporter of the counterregulation-stimulatory amino acid transmitter glutamate (Fig. 3C and D). Results indicate that nNOS siRNA decreased basal Ghrh gene expression in VMNdm [Fig. 3A; $F_{(3,44)}$: 189.75, $p < 0.001$, Knockdown main effect: $F_{(1,44)}$: 29.07; $p < 0.001$; INS main effect: $F_{(1,44)}$: 535.04, $p < 0.001$; Knockdown/INS interaction: $F_{(1,44)}$: 5.14, $p = 0.028$], but not VMNvl GABA neurons [Fig. 3B; $F_{(3,44)}$: 823.68, $p < 0.001$; Knockdown main effect: $F_{(1,44)}$: 834.33, $p < 0.001$; INS main effect: $F_{(1,44)}$: 774.93, $p < 0.001$; Knockdown/INS interaction: $F_{(1,44)}$: 861.78, $p < 0.001$]. Hypoglycemic inhibition of this gene profile was attenuated in each divisional GABA neuron subpopulation by nNOS siRNA pretreatment. Figure 3C and D show that nNOS gene knockdown suppresses basal Slc1a2 mRNA in VMNdm [$F_{(3,44)}$: 196.83, $p < 0.001$; Knockdown main

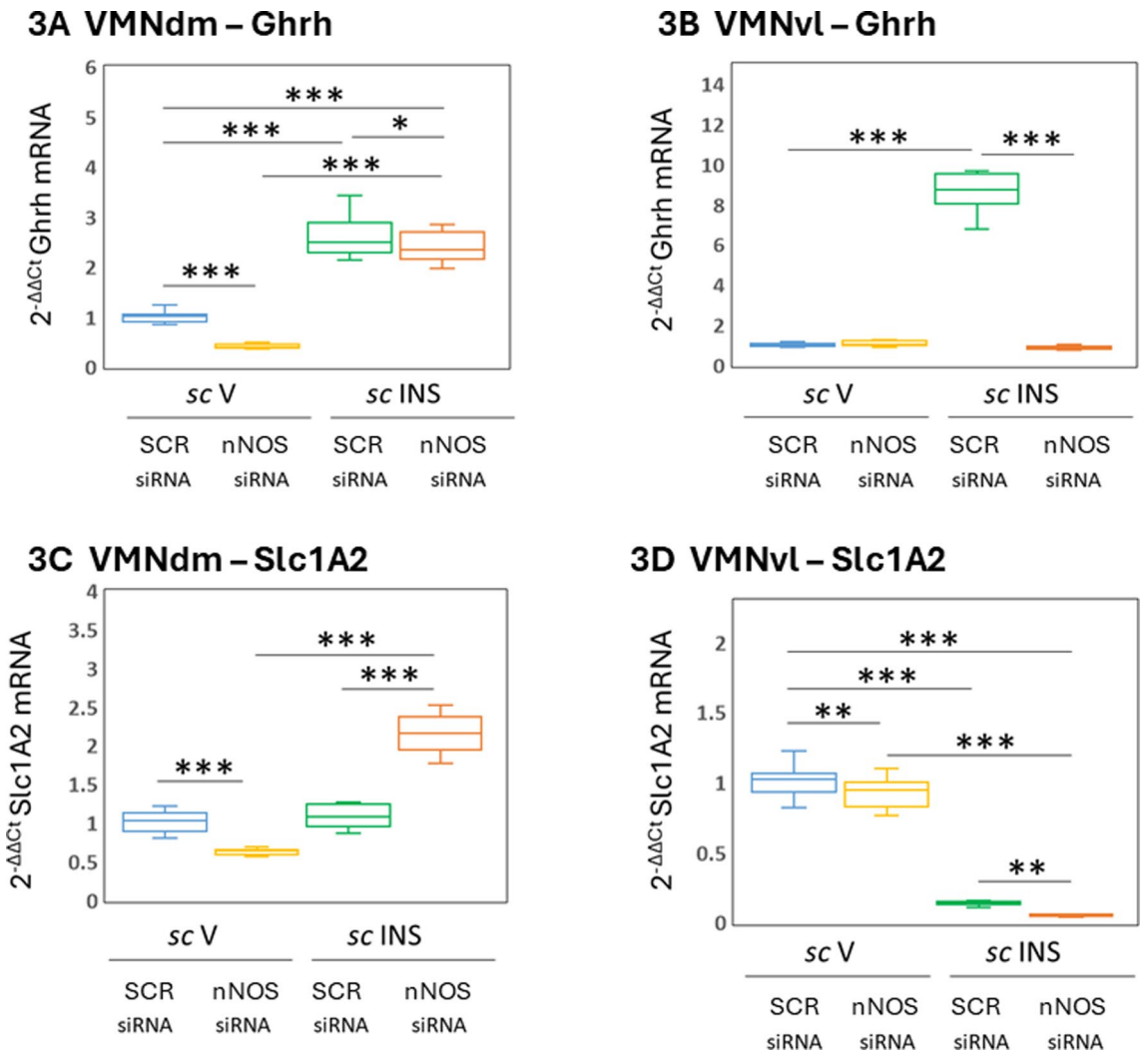

Fig. 3 VMNdm versus VMNvl GABAergic Nerve Cell Co-Expressed Counterregulatory Neurochemical Marker mRNA Content: Effects of VMN nNOS Gene Silencing. Box-and-whisker plots depict normalized values for GABAergic nerve cell mRNAs encoding, growth hormone-releasing hormone (Ghrh), or the vesicular glutamate transporter-1 (Slc1A2), a marker for glutamate. Plots depict normalized Ghrh [Fig. 3**A** (VMNdm) and 3**B** (VMNvl)], or Slc1A2 [Fig. 3**C** (VMNdm) and 3**D** (VMNvl)] values derived from each VMN GABA nerve cell subpopulation neurons for the following treatment groups: SCR siRNA/*sc* V (blue box-and-whisker plots, $n=12$), nNOS siRNA/*sc* V (yellow box-and-whisker plots; $n=12$), SCR siRNA/*sc* INS (green box-and-whisker plots; $n=12$), or nNOS siRNA/*sc* INS (orange box-and-whisker plots; $n=12$). Statistical differences between discrete pairs of treatment groups are indicated by $^{*}p<0.05$; $^{**}p<0.01$; or $^{***}p<0.001$

effect: $F_{(1,44)}$: 52.13, $p<0.001$; INS main effect: $F_{(1,44)}$: 296.26, $p<0.001$; Knockdown/INS interaction: $F_{(1,44)}$: 242.10, $p<0.001$] and VMNvl GABA neurons [$F_{(3,44)}$: 498.95, $p<0.001$; Knockdown main effect: $F_{(1,44)}$: 15.43, $p<0.001$; INS main effect: $F_{(1,44)}$: 1481.41, $p<0.001$; Knockdown/INS interaction: $F_{(1,44)}$: 0.00, $p=0.968$]. IIH had no impact on this gene profile in VMNdm GABA nerve cells but downregulated this mRNA in the VMNvl subpopulation. nNOS siRNA pretreatment amplified Slc1A2 gene transcription in VMNdm GABA neurons collected from INS-injected male rat but intensified hypoglycemic inhibition of gene expression in the VMNvl.

Data in Fig. 4 depict eu- and hypoglycemic patterns of SF-1 gene expression in VMNdm (Fig. 4A) and VMNvl (Fig. 4B) GABA neurons after nNOS gene silencing. Results indicate that nNOS siRNA respectively increased or decreased basal GABA neuron SF-1 mRNA levels in the former [$F_{(3,44)}$: 20.75, $p<0.001$; Knockdown main effect: $F_{(1,44)}$: 45.29, $p<0.001$; INS main effect: $F_{(1,44)}$: 9.82, $p=0.003$; Knockdown/INS interaction: $F_{(1,44)}$: 7.13, $p=0.011$] and latter [$F_{(3,44)}$: 417.28, $p<0.001$; Knockdown main effect: $F_{(1,44)}$: 871.05, $p<0.001$; INS main effect: $F_{(1,44)}$: 252.41, $p<0.001$; Knockdown/INS interaction: $F_{(1,44)}$: 128.38, $p<0.001$] subpopulations. IIH had discrepant effects on SF-1 gene expression in the two GABA nerve cell groups, as this gene profile was respectively

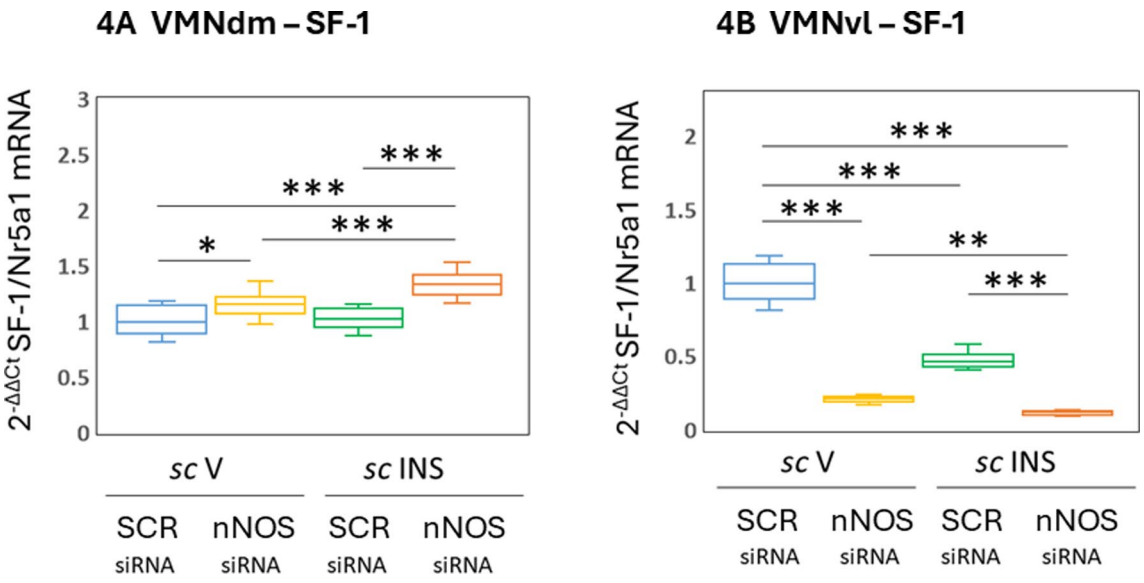

Fig. 4 Impact of VMN nNOS Gene Silencing on Eu- and Hypoglycemic Patterns of Steroidogenic Factor-1 (SF-1)/Nr5a1 mRNA Expression in VMN Division-Based GABA Neuron Subpopulations. Plots depict normalized Nr5a1/SF-1 [Fig. 4**A** (VMNdm) and 4**B** (VMNvl)] mRNA measures for GABA neurons collected from SCR siRNA/*sc* V (blue box-and-whisker plots, $n = 12$), nNOS siRNA/*sc* V (yellow box-and-whisker plots; $n = 12$), SCR siRNA/ *sc* INS (green box-and-whisker plots; $n = 12$), or nNOS siRNA/*sc* INS (orange box-and-whisker plots; $n = 12$) treatment groups. Statistical differences between discrete pairs of treatment groups are indicated by the following symbols: *$p < 0.05$; **$p < 0.01$; ***$p < 0.001$

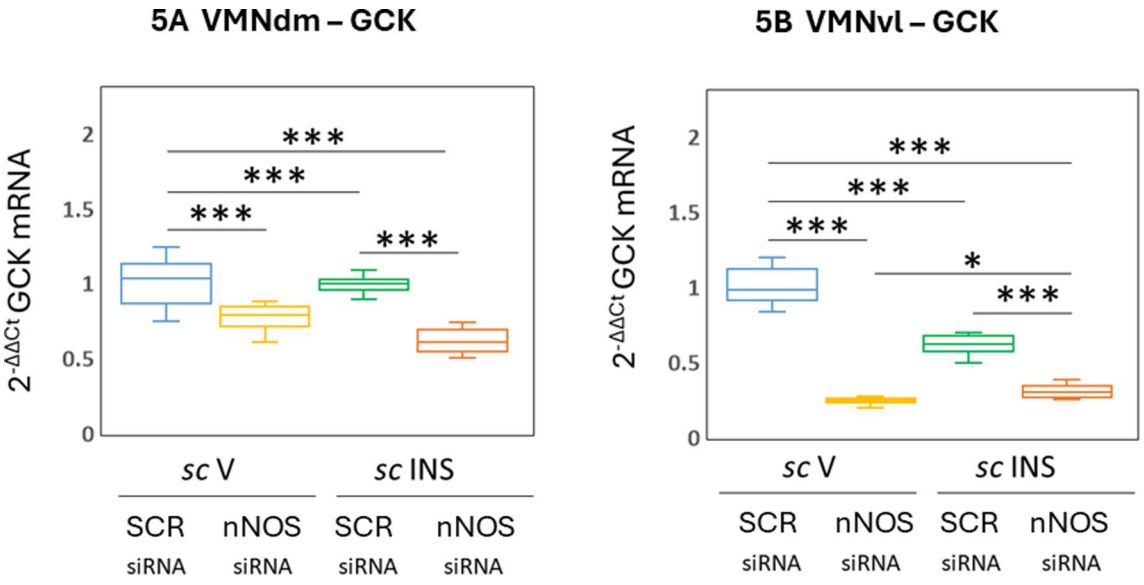

Fig. 5 VMN nNOS Gene Knockdown Effects on VMNdm versus VMNvl GABAergic Nerve Cell Glucokinase (GCK) mRNA Levels in Eu- or Hypoglycemic Male Rats. Individual VMNdm and VMNvl GAD-ir neurons were harvested by laser-catapult-microdissection for multiplex gene expression analysis including GLUT2. Plots depict normalized GLUT2 [Fig. 5**A** (VMNdm) and 5**B** (VMNvl)] mRNA measures for GABA neurons acquired from the following treatment groups: SCR siRNA/*sc* V (blue box-and-whisker plots, $n = 12$), nNOS siRNA/*sc* V (yellow box-and-whisker plots; $n = 12$), SCR siRNA/ *sc* INS (green box-and-whisker plots; $n = 12$), nNOS siRNA/*sc* INS (orange box-and-whisker plots; $n = 12$). Statistical differences between discrete pairs of treatment groups are indicated by the following symbols: *$p < 0.05$; **$p < 0.01$; ***$p < 0.001$

unchanged (VMNdm) or decreased (VMNvl) after INS injection. nNOS siRNA pretreatment had divergent effects on hypoglycemic patterns of SF-1 gene transcription as this mRNA was correspondingly increased or decreased in GABA neurons collected from the VMNdm versus VMNvl of INS-injected male rats.

Figure 5 illustrates effects of VMN nNOS gene knockdown on GABAergic neuron GCK gene expression. Data show that the VMNdm cell group (Fig. 5A) showed down-regulation of this baseline gene profile after nNOS siRNA administration [$F_{(3,44)}$: 44.52, $p < 0.001$; Knockdown main effect: $F_{(1,44)}$: 118.39, $p < 0.001$; INS main

effect: $F_{(1,44)}$: 9.62, $p = 0.003$; Knockdown/INS interaction: $F_{(1,44)}$: 5.86, $p = 0.020$]. Hypoglycemic inhibition of VMNdm GABA neuron GCK gene transcription was intensified by nNOS siRNA pretreatment. nNOS gene knockdown inhibited VMNvl GABAergic neuron (Fig. 5B) [$F_{(3,44)}$: 280.50, $p < 0.001$; Knockdown main effect: $F_{(1,44)}$: 660.06, $p < 0.001$; INS main effect: $F_{(1,44)}$: 62.41, $p < 0.001$; Knockdown/INS interaction: $F_{(1,44)}$: 119.04, $p < 0.001$] baseline GCK gene expression, and exacerbated hypoglycemic down-regulation of this gene profile.

Data in Fig. 6 depict eu- and hypoglycemic patterns of AMPKα1 and AMPKα2 gene expression in VMNdm versus VMNvl GABAergic neurons following VMN nNOS gene knockdown. As shown in Fig. 6A and B, this gene silencing paradigm had divergent effects on baseline AMPKα1 mRNA levels as this gene profile was respectively up- or down-regulated in VMNdm [$F_{(3,44)}$: 121.61, $p < 0.001$; Knockdown main effect: $F_{(1,44)}$: 55.64, $p < 0.001$; INS main effect: $F_{(1,44)}$: 186.74, $p < 0.001$; Knockdown/INS interaction: $F_{(1,44)}$: 122.45, $p < 0.001$] versus VMNvl GABA nerve cells taken from V-injected male rats [$F_{(3,44)}$: 476.37, $p < 0.001$; Knockdown main effect: $F_{(1,44)}$: 1248.41, $p < 0.001$; INS main effect: $F_{(1,44)}$: 138.85, $p < 0.001$; Knockdown/INS interaction: $F_{(1,44)}$: 41.86, $p < 0.001$]. GABA nerve cell AMPKα1 gene profiles were refractory to (VMNdm) or increased (VMNvl) in response to IIH. nNOS siRNA pretreatment suppressed AMPKα1 transcription in both GABA neuron subpopulations after INS injection. Figure 6C and D shown that VMN nNOS gene silencing did not modify baseline VMNdm GABA neuron AMPKα2 gene expression [$F_{(3,44)}$: 19.61, $p < 0.001$;

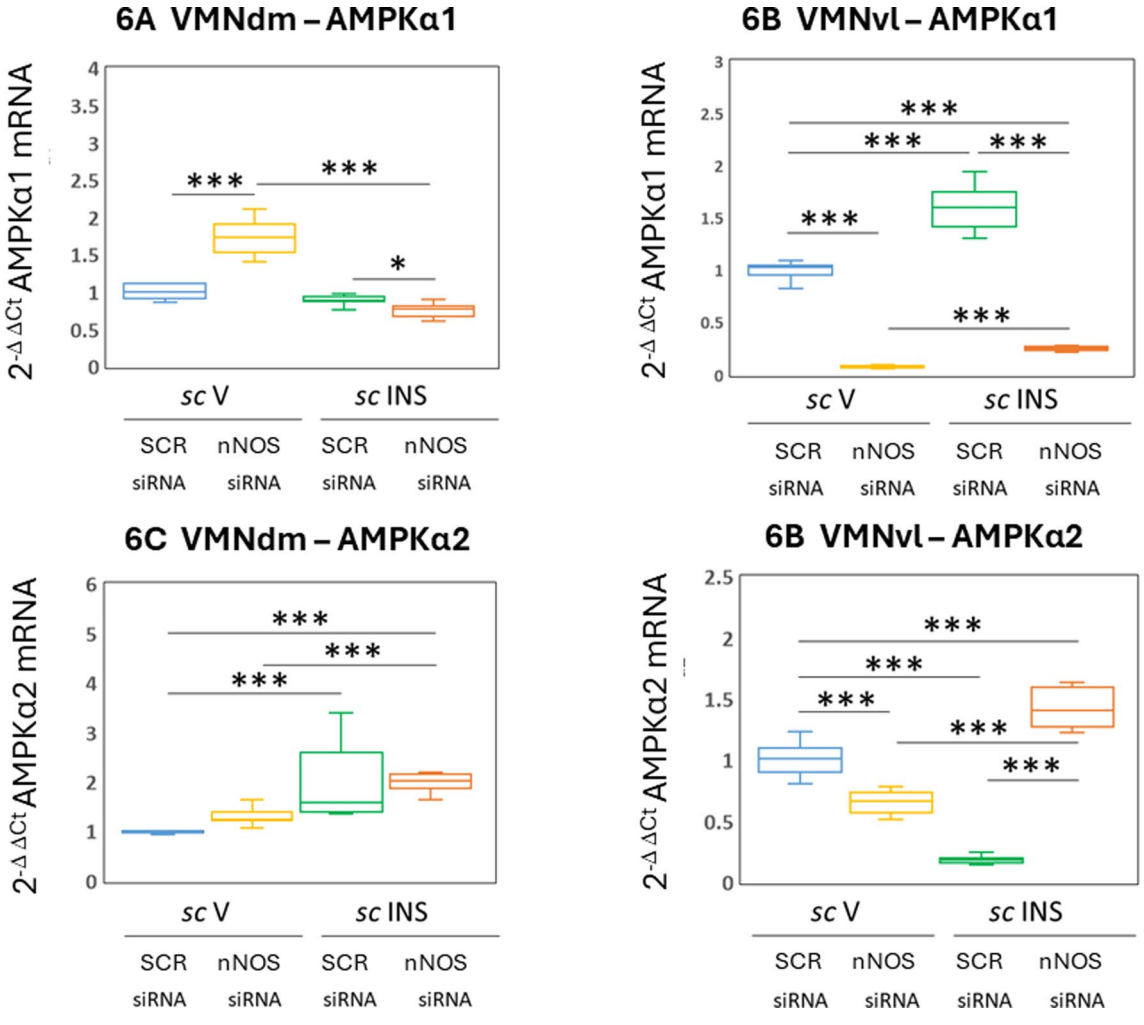

Fig. 6 Effects of VMN nNOS siRNA Pretreatment on Eu- and Hypoglycemic Patterns of 5′-AMP-Activated Protein Kinase-Alpha1 (AMPKα1) and AMPKα2 Gene Expression in VMNdm versus VMNvl GABAergic Neurons. Plots depict normalized AMPKα1 [Fig. 6**A** (VMNdm) and 6**B** (VMNvl)] or AMPKα2 [Fig. 6**C** (VMNdm) and 6**D** (VMNvl)] mRNA measures for GABA neurons collected from SCR siRNA/*sc* V (blue box-and-whisker plots, $n = 12$), nNOS siRNA/*sc* V (yellow box-and-whisker plots; $n = 12$), SCR siRNA/ *sc* INS (green box-and-whisker plots; $n = 12$), or nNOS siRNA/*sc* INS (orange box-and-whisker plots; $n = 12$) treatment groups. Statistical differences between discrete pairs of treatment groups are indicated by the following symbols: $^{*}p < 0.05$; $^{**}p < 0.01$; $^{***}p < 0.001$

Knockdown main effect: $F_{(1,44)}$: 2.97, $p = 0.092$; INS main effect: $F_{(1,44)}$: 54.69, $p < 0.001$; Knockdown/INS interaction: $F_{(1,44)}$: 1.17, $p = 0.285$] but diminished this gene profile in the VMNvl cell group [$F_{(3,44)}$: 249.90, $p < 0.001$; Knockdown main effect: $F_{(1,44)}$: 174.16; $p < 0.001$; INS main effect: $F_{(1,44)}$: 0.63, $p = 0.433$; Knockdown/INS interaction: $F_{(1,44)}$: 574.92; $p < 0.001$]. IIH had opposite effects on AMPKα2 gene expression in the two VMN GABA cell groups; data show that this mRNA profile was increased or decreased in VMNdm versus VMNvl subpopulations. nNOS siRNA pretreatment did not affect IIH-associated AMPKα2 gene transcription in VMNdm GABA neurons but reversed hypoglycemic inhibition of this gene profile in VMNvl cells.

Data in Fig. 7 illustrates effects of VMN nNOS gene knockdown on GABAergic neuron GLUT2 (Fig. 7A and B) and GLUT3 (Fig. 7C and D) gene expression following V- or INS-injection. VMNdm [$F_{(3,44)}$: 258.57, $p < 0.001$; Knockdown main effect: $F_{(1,44)}$: 743.41, $p < 0.001$; INS main effect: $F_{(1,44)}$: 22.03, $p < 0.001$; Knockdown/INS interaction: $F_{(1,44)}$: 10.29, $p = 0.002$] and VMNvl [$F_{(3,44)}$: 463.21, $p < 0.001$; Knockdown main effect: $F_{(1,44)}$: 1301.78, $p < 0.001$; INS main effect: $F_{(1,44)}$: 20.39, $p < 0.001$; Knockdown/INS interaction: $F_{(1,44)}$: 67.46; $p < 0.001$] GABA neurons each shown down-regulated baseline GLUT2 gene expression in response to nNOS gene knockdown. IIH did not modify this gene profile in VMNdm neurons, but inhibited GLUT2 mRNA in the VMNvl cell

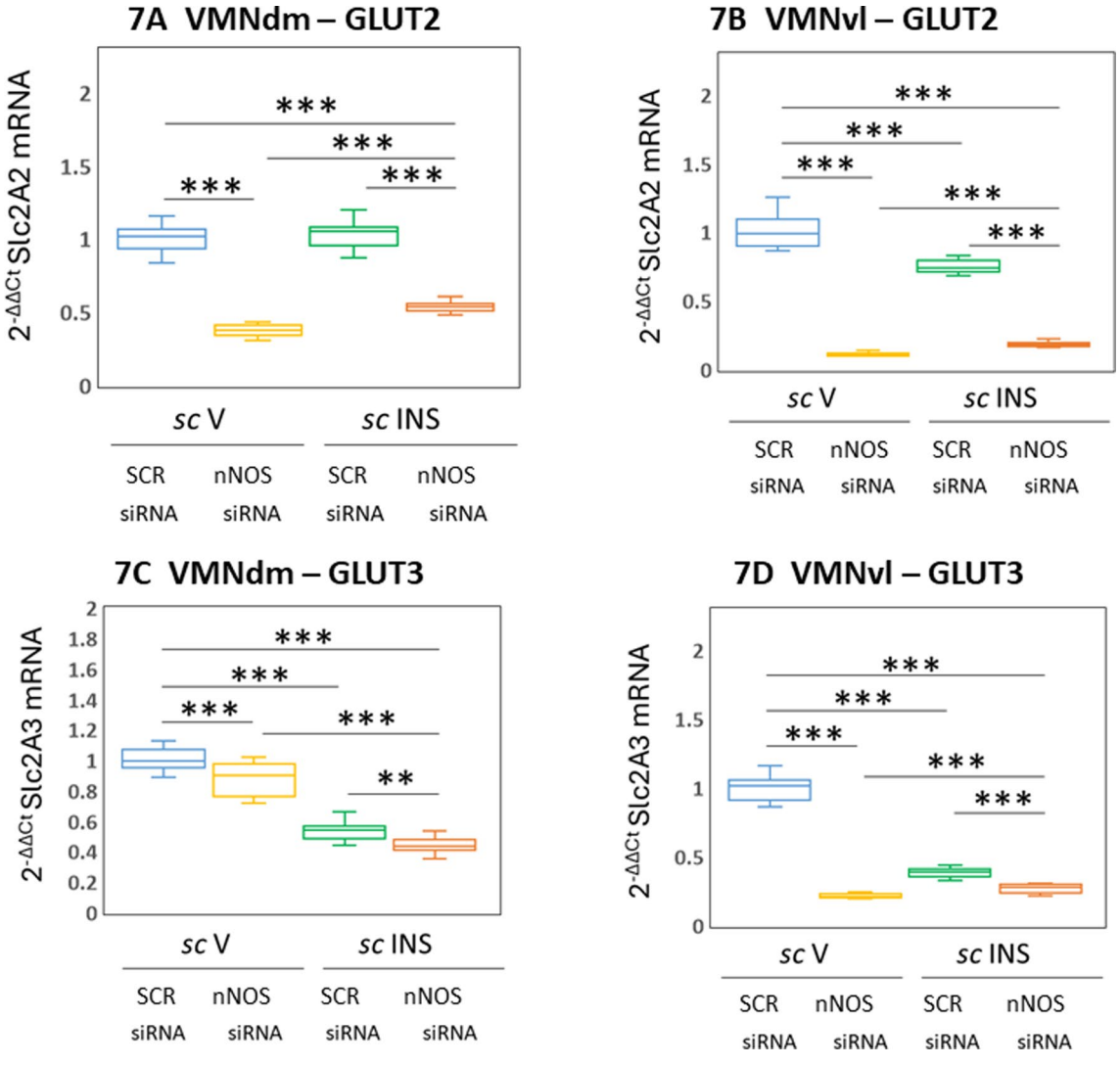

Fig. 7 VMN nNOS siRNA Effects on VMNdm versus VMNvl GABA Neuron Glucose Transporter-2 (GLUT2) and Glucose Transporter-3 (GLUT3) Gene Expression. Individual laser-catapult-microdissected VMNdm or VMNvl GAD-ir neurons from SCR siRNA/*sc* V (blue box-and-whisker plots, $n = 12$), nNOS siRNA/*sc* V (yellow box-and-whisker plots; $n = 12$), SCR siRNA/ *sc* INS (green box-and-whisker plots; $n = 12$), or nNOS siRNA/*sc* INS (orange box-and-whisker plots; $n = 12$) treatment groups were analyzed by multiplex qPCR for GLUT2 and GLUT3 gene expression. Plots depict normalized GLUT2 [Fig. 7**A** (VMNdm) and 7**B** (VMNvl)] or GLUT3 [Fig. 7**C** (VMNdm) and 7**D** (VMNvl)] mRNA measures for each GABA nerve cell subpopulation. Statistical differences between discrete pairs of treatment groups are indicated by the following symbols: *$p < 0.05$; **$p < 0.01$; ***$p < 0.001$

group. nNOS siRNA pretreatment decreased GLUT2 gene transcription in GABA neurons collected from either VMN location after INS injection. Figure 7C and D show that nNOS gene knockdown likewise down-regulated GLUT3 gene profiles in VMNdm [$F_{(3,44)}$: 137.37, $p < 0.001$; Knockdown main effect: $F_{(1,44)}$: 24.89, $p < 0.001$; INS main effect: $F_{(1,44)}$: 386.98, $p < 0.001$; Knockdown/INS interaction: $F_{(1,44)}$: 0.25, $p = 0.619$] and VMNvl [$F_{(3,44)}$: 588.89, $p < 0.001$; Knockdown main effect: $F_{(1,44)}$: 904.99, $p < 0.001$; INS main effect: $F_{(1,44)}$: 353.24, $p < 0.001$; Knockdown/INS interaction: $F_{(1,44)}$: 508.44, $p < 0.001$] GABA neurons. IIH inhibited GLUT3 gene expression in both GABA nerve cell groups; this inhibitory transcriptional response was amplified by nNOS siRNA pretreatment.

Data in Fig. 8 disclose effects of VMN nNOS gene silencing on GABAergic nerve cell GPR81 gene expression in eu- or hypoglycemic male rats. This genetic manipulation had opposite effects on baseline GPR81 mRNA levels; this gene profile was increased [VMNdm; $F_{(3,44)}$: 59.42, $p < 0.001$; Knockdown main effect: $F_{(1,44)}$: 104.17, $p < 0.001$; INS main effect: $F_{(1,44)}$: 73.57, $p < 0.001$; Knockdown/INS interaction: $F_{(1,44)}$: 0.51, $p = 0.479$] or decreased [VMNvl; $F_{(3,44)}$: 1115.98, $p < 0.001$; Knockdown main effect: $F_{(1,44)}$: 1166.11, $p < 0.001$; INS main effect: $F_{(1,44)}$: 1099.67, $p < 0.001$; Knockdown/INS interaction: $F_{(1,44)}$: 1082.16, $p < 0.001$] in response to intra-VMN nNOS siRNA administration. While GPR81 gene expression was downregulated in both GABA cell groups in response to IIH, nNOS siRNA pretreatment prevented this inhibitory response in VMNdm neurons, but did not affect transcriptional activity in VMNvl GABA neurons.

Outcomes depicted in Fig. 9 illustrate effects of VMN NO gene silencing on peripheral glucose and counter-regulatory hormone profiles. Figure 9A shows that nNOS siRNA significantly elevated plasma glucose levels in V-injected control male rats [$F_{(3,20)}$: 257.20, $p < 0.001$; Knockdown main effect: $F_{(1,20)}$: 12.19, $p = 0.002$; INS main effect: $F_{(1,20)}$: 756.71, $p < 0.001$; Knockdown/INS interaction: $F_{(1,20)}$: 2.69, $p = 0.117$]. INS injection caused comparable reductions in plasma glucose levels in SCR versus nNOS siRNA-pretreated groups. Data in Fig. 9B indicate that VMN nNOS gene knockdown increased circulating glucagon concentrations in euglycemic animals [$F_{(3,20)}$: 213.76, $p < 0.001$; Knockdown main effect: $F_{(1,20)}$: 163.62, $p < 0.001$; INS main effect: $F_{(1,20)}$: 149.61, $p < 0.001$; Knockdown/INS interaction: $F_{(1,20)}$: 328.04, $p < 0.001$]. Conversely, this genetic manipulation significantly attenuated hypoglycemic up-regulation of this hormone profile. Figure 9C shows that basal plasma corticosterone levels were elevated in response to VMN nNOS siRNA [$F_{(3,20)}$: 89.96, $p < 0.001$; Knockdown main effect: $F_{(1,20)}$: 26.47, $p < 0.001$; INS main effect: $F_{(1,20)}$: 79.18, $p < 0.001$; Knockdown/INS interaction: $F_{(1,20)}$: 164.23, $p < 0.001$]. INS-injected rats pretreated with nNOS siRNA showed a significant reduction in circulating corticosterone levels compared to the SCR siRNA/INS treatment group.

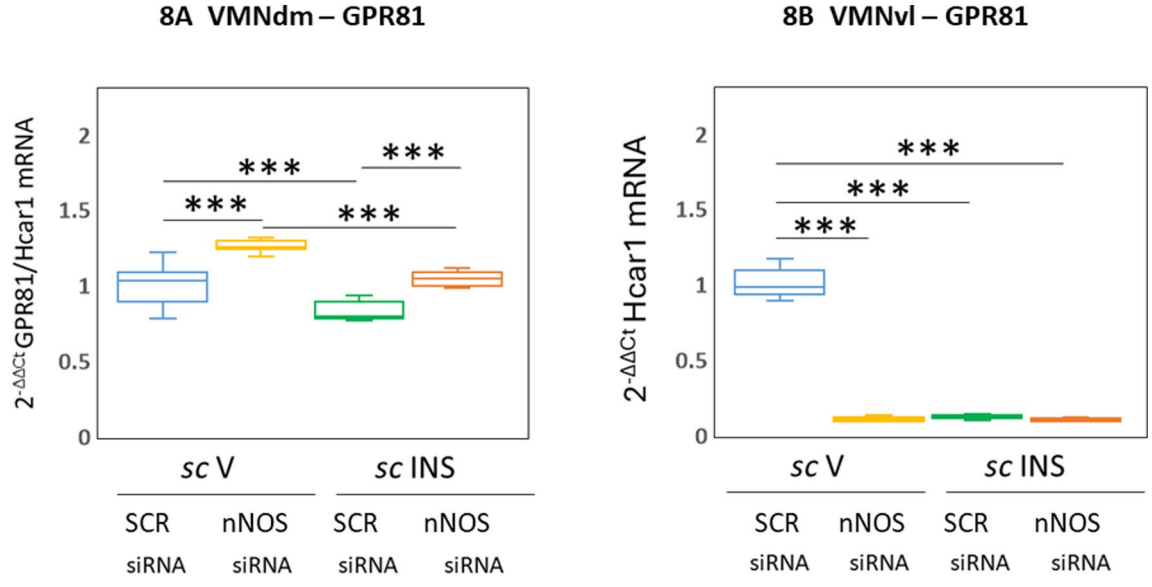

Fig. 8 Effects of VMN nNOS siRNA Pretreatment on Eu- and Hypoglycemic Patterns of G-Protein-Coupled-81 (GPR81) Gene Expression in VMNdm versus VMNvl GABAergic Neurons. Plots depict normalized GPR81 [Fig. 8**A** (VMNdm) and 8**B** (VMNvl)] for GABAergic nerve cells acquired from subjects in the following treatment groups: SCR siRNA/*sc* V (blue box-and-whisker plots, $n = 12$), nNOS siRNA/*sc* V (yellow box-and-whisker plots; $n = 12$), SCR siRNA/ *sc* INS (green box-and-whisker plots; $n = 12$), or nNOS siRNA/*sc* INS (orange box-and-whisker plots; $n = 12$) treatment groups. Statistical differences between individual pairs of treatment groups are indicated by the following symbols: *$p < 0.05$; **$p < 0.01$; ***$p < 0.001$

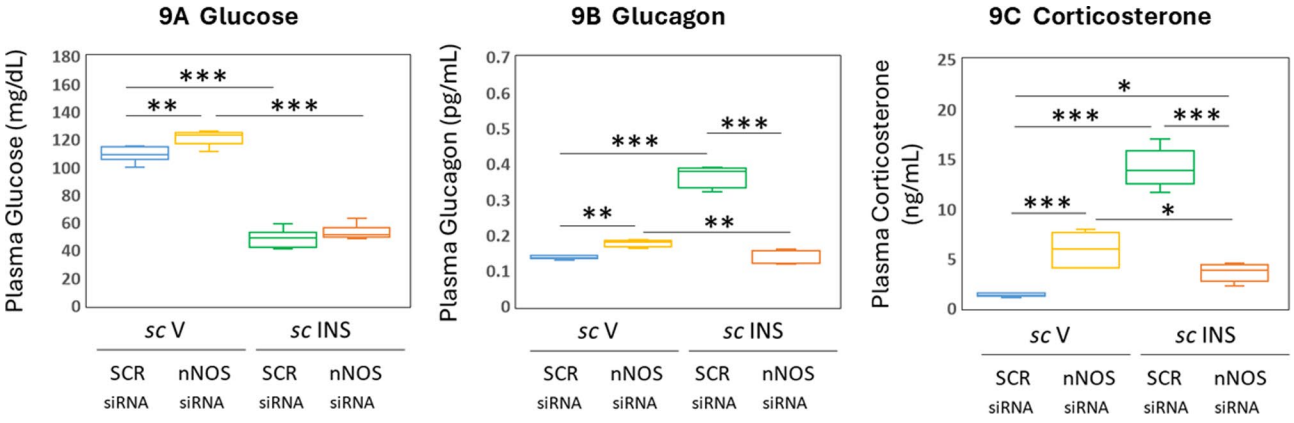

Fig. 9 Effects of VMN nNOS Gene Knockdown on Circulating Glucose and Counterregulatory Hormone Profiles in the Adult Male Rat. Box-and-Whisker plots depict plasma glucose (Fig. 9**A**), glucagon (Fig. 9**B**), or corticosterone (Fig. 9**C**) concentrations for the following treatment groups: SCR siRNA/*sc* V (blue box-and-whisker plots, $n=6$), nNOS siRNA/*sc* V (yellow box-and-whisker plots; $n=6$), SCR siRNA/ *sc* INS (green box-and-whisker plots; $n=6$), or nNOS siRNA/*sc* INS (orange box-and-whisker plots; $n=6$) treatment groups. Statistical differences between discrete pairs of treatment groups are indicated by the following symbols: *$p<0.05$; **$p<0.01$; ***$p<0.001$

Discussion

The diffusible neurotransmitter NO purportedly acts on unknown cellular targets in the male rat MBH to optimize IIH-associated counterregulatory hormone outflow in that sex. Current research utilized in vivo site-targeted nNOS gene silencing and single-cell laser-catapult-microdissection/multiplex qPCR methods to investigate the following related premises: (1) VMN NO may be critical to neural control of this endocrine outflow, and (2) locally-generated NO may control metabolic sensory and neurotransmitter functions in one or more VMN GABAergic neuron units under conditions of glucose sufficiency and/or deficiency. Results provide unexpected evidence for bi-directional, glucose status-specific VMN NO regulation of glucagon and corticosterone secretion in male rats, as VMN nNOS gene knockdown respectively up- or down-regulated release of these hormones in V- versus INS-injected animals. Single-cell multiplex gene expression analysis showed that IIH increased nNOS mRNA in VMNdm and VMNvl GABA cell groups. Pretreatment with nNOS siRNA affected IIH-associated transcription of common as well as unique metabolic sensor and counterregulatory neurochemical marker genes in these GABAergic neuron populations. Further studies are needed to identify the molecular mechanisms for glucose-dependent directional shift in VMN NO control of counterregulatory hormone secretion in male rats, and to determine if and how NO-dependent patterns of counterregulation-enhancing and -constraining neurotransmitter signaling by VMNdm versus VMNvl GABA neurons may impact neural control of counterregulatory hormone secretion.

Study outcomes are important for identifying the VMN as a site of NO control of glucose counterregulation in the male rat, and for delineating discrete GABAergic neuron groups as potential targets for this regulatory action. Present data confirm VMN GABA neuron co-transmission of counterregulation-restraining and -enhancing neurotransmitters of different chemical structure and temporo-spatial release profiles, inferring that this nerve cell type may provide complex integrated input to downstream targets within the brain glucostasis network. Notably, current work advances the novel concept that NO released by VMN GABAergic neurons may operate as an autocrine regulatory signal, thereby imposing discriminative control of neurotransmitter gene profiles in VMNdm versus VMNvl subgroups. Ongoing research seeks to determine if NO-dependent counterregulatory neurochemical signals released by each GABA neuron subpopulation communicate, alone or in combination, unique information on brain cell energy state, metabolic fuel, i.e. lactate and glucose supply, or local or peripheral energy reserve capacities, such as brain or liver glycogen and adipose tissue volume. NO acts by a canonical pathway that involves receptor-coupled soluble guanylyl cyclase (sGC)stimulation of cyclic GMP production [8]. Further effort is needed to determine if VMNdm and VMNvl GABA neurons express sGC; forthcoming evidence that one or both subpopulations lack this enzyme would infer that NO may regulate transcriptional activity in those cell units by non-canonical mechanisms of action or, alternatively, by indirect means via afferent input from neurons subject to NO paracrine control. The possibility that VMN NO control of peripheral counterregulatory hormone profiles may involve integrated neurotransmission by multiple VMN neuron populations, as opposed to a singular role for GABAergic neurons, should not be discounted. As quantification of NO production by individual GABA nerve cells under eu- versus hypoglycemic conditions or establishment of tissue NO

concentrations between cellular point of origin and diffusion limit were beyond the scope of current research, the identity and number of neighboring NO-sensitive neurons remain speculative. Outcomes here do not identify the stimulatory signal(s) that up-regulates VMNdm and VMNvl GABA neuron nNOS gene expression during IIH. It should be noted that measurable changes in gene transcripts of interest, including nNOS mRNA, do not affirm that parallel adjustments in gene protein product expression occur. While it is reasonable to surmise that nNOS gene siRNA-associated changes in distinctive mRNA profiles may likely affect translatable protein yield, confirmation of this stance will require application of as-yet-unavailable analytical tools of requisite sensitivity for quantification of target protein in single brain cell samples. It should also be noted that alterations in enzyme protein profiles are not definitive proof of corresponding changes in enzyme activity.

The enzyme GAD catalyzes the rate-limiting step in GABA biosynthesis, i.e., derivation from its immediate metabolic precursor glutamate. GAD occurs as two molecular weight variants GAD1/GAD_{67} (67 kDa) and GAD2/GAD_{65} (65 kDa) in the brain, encoded by separate genes. Our studies show that VMN $GAD_{65/67}$-ir neurons co-express GAD1 and GAD2 mRNAs [Ali et al., 2022]. These enzyme isoforms exhibit differences in primary amino acid structure, neuron subcellular distribution, and physiological regulation [33]. Differential GAD2/GAD_{65} (axon terminals/vesicles) versus GAD1/GAD_{67} (cytoplasm) localization infers that distinctive intra-cellular GABA pools participate in neurotransmission or cellular metabolic functions, respectively [34–36]. GAD1 exhibits constitutive activity and generates a large percentage of brain GABA, whereas GAD2 is transiently activated to augment GABA levels for rapid inhibitory neurotransmission [37, 38]. GAD1 involvement in GABA synaptic release is supported by evidence that membrane anchoring of this enzyme isoform results in axonal targeting and presynaptic clustering that facilitates GABA accumulation for axon terminal rapid discharge [39]. An intriguing alternative prospect is that GAD1 may play a role in documented unconventional GABA release, achieved by mechanisms that include reversal of transporter activity or other non-vesicular means, at sites outside axon terminals [40]. Current data infer that NO stimulates basal GAD1 and GAD2 gene expression in each GABA nerve cell unit but imposes division-specific control of these gene profiles during IIH. Whereas NO likely imposes a positive regulatory tone on VMNvl GAD isoform mRNAs during IIH, thereby blunting transcript diminution, this neurotransmitter may simultaneously direct the inhibitory VMNdm GAD1 transcriptional response to IIH while GAD2 mRNA in that cell group is refractory to NO. Notably, glucose status apparently affects nitrergic regulation of VMNdm GAD gene expression as the direction of control of GAD1 switches from stimulatory (euglycemia)-to-inhibitory (IIH) and IIH causes a loss of NO regulation of GAD2 gene profiles. There is evident need to characterize the molecular mechanisms that implement these metabolic-dependent adjustments in nitrergic control of GAD mRNA profiles in this specific GABA neuron subpopulation. Disparate eu- versus IIH-associated NO effects in that cell group may reflect, in part, differences in neurotransmitter signal volume; alternatively, metabolic cues may shape direction of or abolish canonical and/or non-canonical pathway regulation of GAD1 or GAD2 gene transcription, respectively. It will be important to identify the metabolic stimuli that enact that control and to determine if these signals originate within and/or outside this GABA cell subpopulation.

The neuropeptide Ghrh and amino acid glutamate enhance counterregulatory hormone outflow [5, 41]. VMNdm and VMNvl $GAD_{65/67}$-ir neurons express transcripts that produce Ghrh and the glutamate marker vesicular glutamate transporter Slc1A2/GLT-1 [7]. Present data infer that NO regulation of baseline Ghrh gene expression varies between VMNdm and VMNvl GABA neurons as nNOS siRNA down-regulates this gene profile in the former, but not latter cell unit. Yet, NO evidently drives IIH-associated augmentation of Ghrh transcription in both subpopulations, indicative of a gain of NO regulatory control of this gene profile in VMNvl GABA nerve cells. While NO is stimulatory to baseline VMNdm and VMNvl GABA neuron Slc1A2 gene expression, control of Slc1A2 mRNA profiles during IIH differs between the two cell groups as tone switches from stimulatory-to-inhibitory in former yet offsets inhibition of Slc1A2 gene expression in the latter subpopulation. Taken together, these findings infer that NO may generally facilitate basal transmission of these counterregulation-augmenting neurochemicals and may be required for optimal IIH-associated up-regulated Ghrh gene transcription in VMNdm and VMNvl GABAergic nerve cells.

Over the whole brain, the metabolic nuclear transcription factor SF-1 is expressed exclusively in the VMN, where it reportedly occurs primarily in dorsomedial and central VMN divisions [42, 43]. Current data show that VMNdm and VMNvl GABAergic neurons express mRNA that encodes SF-1. These disparate outcomes could reflect, in part, differences in experimental methods, including analytical tools for quantification of SF-1 gene expression, tissue sampling and processing techniques, and animal models. It should be kept in mind that SF-1 mRNA analysis was performed on phenotypically characterized nerve cell samples. Data here show that NO evidently exerts opposite regulatory effects on SF-1 gene transcription in the two GABA nerve cell

groups during eu- and hypoglycemia, i.e., inhibitory to VMNdm neuron SF-1 mRNA profiles versus stimulatory to this gene profile in VMNvl cells. Interestingly, IIH had unlike effects on SF-1 gene expression in VMNdm versus VMNvl GABA neurons as these transcripts were respectively refractory to or were diminished by this metabolic challenge in the former and latter cell groups. These findings infer that cellular responses to IIH may be SF-1 -dependent versus -independent in these division-based subpopulations.

Present evidence that VMNdm and VMNvl GABAergic neurons express GCK mRNA implicates these distinctive cell groups in intracellular glucose monitoring. Data document NO stimulation of this gene profile during eu- and hypoglycemia, indicating that this signal blunts downregulation under the latter circumstances. Although the mechanisms that underlie IIH-associated suppression of this GCK transcription are unclear, this response is plausibly a NO-sensitive adaptation to decreased intracellular glucose. AMPKα1 and −2 gene expression points to a metabolic sensory function of VMNdm and VMNvl GABA neurons. Interestingly, IIH caused division-specific adjustments in these catalytic subunit mRNA profiles as AMPKα1 transcription was unaffected (VMNdm) or increased (VMNvl) while AMPKα2 transcripts were amplified (VMNdm) or diminished (VMNvl). Current data reveal subpopulation-specific NO control of euglycemic patterns of AMPK alpha subunit gene transcription as VMNdm AMPKα1 gene expression was up-regulated by nNOS gene silencing yet this genetic manipulation diminished each AMPK alpha subunit mRNA in the VMNvl cell group. It should be noted that the direction of NO regulation of VMNdm AMPKα1 and VMNvl AMPKα2 gene profiles varies between eu- versus hypoglycemia, as this control shifts from inhibitory to stimulatory in the former instance and from stimulatory to inhibitory in regard to the latter gene profile.

The unique functional attributes of the glucose transporter GLUT2 infer that it likely operates as a glucose sensor at the interface between extra- and intracellular environments [13, 14]. Current studies affirm prior reports that GCK and GLUT2 co-exist in vivo in hypothalamic neurons [44, 45] and advance those findings through identification of a VMN counterregulatory neurochemical phenotype which expresses both gene transcripts. Our data show that NO is a positive stimulus for VMN GABA neuron GLUT2 transcription under eu- and hypoglycemic conditions. The notable discovery here is that IIH down-regulates GLUT2 mRNA in VMNvl, but not VMNdm GABAergic neurons. Within the context of the presumption that IIH causes an equivalent reduction in tissue glucose levels in each VMN division, closer alignment of GLUT2 gene expression in the VMNvl cell group to decreased glucose provision may signify dissimilar sensory functionality between the two subpopulations. IIH-associated downregulation of the constitutive glucose transporter GLUT3 in GABA neurons in each VMN division likely reflects cellular adaptation to diminished tissue glucose concentrations. Outcomes reveal differential NO regulation of GPR81 gene transcription in VMNdm versus VMNvl GABAergic neurons. This labile neurochemical evidently imposes a negative tone on basal mRNA levels and may be required for hypoglycemic suppression of this gene profile in the former cell group; at the same time, NO serves as a positive stimulus for basal GPR transcription in VMNvl GABA neurons. Notably, NO control of this lactate membrane receptor gene profile is glucose status-specific in the VMNvl cell group as IIH abolishes GPR81 mRNA responsiveness to this signal. Present work does disclose the identity of the regulatory cue(s) that suppresses VMNvl GABA neuron GPR81 gene expression under those conditions. Data here show that IIH downregulates these transcripts in each GABA nerve cell group, a response that could be construed as adaptive downregulation due to diminished receptor ligand; thus, both subpopulations may engage in monitoring of this critical metabolic fuel by NO-dependent (VMNdm) versus -independent (VMNvl) mechanisms. The signal transduction pathway(s) that convey potential downstream effects of GPR81 activation on GABA nerve cell responsiveness to IIH remain to be elucidated.

Current studies document unanticipated bi-directional VMN NO control of glucagon and corticosterone secretion in the male rat. Data infer that this neurochemical operates within that structure to inhibit release of both hormones during euglycemia yet is required for optimal up-regulation of both peripheral profiles during IIH. Augmented secretory patterns following nNOS siRNA administration likely reflects, in part, decreased GAD isoform gene transcription and consequent synthesis and release of the counterregulation-constraining neurotransmitter GABA. Neither Ghrh nor glutamate signals are likely involved in this stimulatory response as both Ghrh and Slc1A2 mRNAs are decreased by nNOS gene silencing. Attenuating effects of nNOS siRNA pretreatment on IIH-associated glucagon and corticosterone outflow patterns may result from reversal of hypoglycemic downregulation of VMNdm GAD1 gene transcription, as well as blunting (VMNdm) or inhibition (VMNvl) of the counterregulatory-enhancing neuropeptide Ghrh and exacerbation of VMNvl glutamate signaling. This interpretation is speculative at present and will require additional research to confirm that one or more of the nNOS siRNA-sensitive neurochemicals discussed above operate within the glucostatic neural network to control counterregulatory hormone secretion during eu- and/or hypoglycemia.

The post-injection time point used here corresponds to the hypoglycemic nadir achieved by subcutaneous administration of the current neutral protamine Hagedorn insulin dose, a dosage that elicits maximum nerve cell transcriptional activation in hypothalamic glucose-regulatory structures. Thus, VMN GABAergic nerve cell target gene transcriptional responses described here arguably reflect, in part, reactivity to maximum glycemic decline achieved by the intermediate insulin formulation used here to our in vivo whole-animal model. However, it is acknowledged that current outcomes do not eliminate the possibility that gene profile readouts may undergo change due to central actions of NPH insulin injection alone or in combination with nNOS siRNA pretreatment. Additional experimentation involving pharmacological agents designed to lower circulating glucose levels by mechanisms independent of insulin action, i.e. augmented kidney clearance, would be useful to understand effects of hypoglycemia alone on VMN GABAergic neuron target gene expression.

In summary, current research addressed the premise that VMN NO action shapes basal and/or hypoglycemic counterregulatory hormone secretion patterns in the male rat, and that NO may regulate metabolic and counterregulatory transmitter marker gene expression in VMNdm and/or VMNvl GABAergic neurons. Study outcomes disclose bi-directional, glucose status-dependent VMN NO control of glucagon and corticosterone secretion in this sex. Multiplex qPCR analysis of laser-catapult-microdissected GABA neurons indicates that nNOS gene expression is upregulated by IIH in VMNdm and VMNvl subpopulations, and that NO regulates common as well as unique transcriptional responses by these cell groups to hypoglycemia. Data support the possibility that in the male, hypoglycemic patterns of NO signaling may modulate distinctive sources of regulatory sensory cues in each GABAergic nerve cell population, which may in turn shape characteristic counterregulatory neurochemical signaling by those cells.

Abbreviations

AMPKα1	5′-AMP-activated protein kinase-alpha1
AMPKα2	5′-AMP-activated protein kinase-alpha2
GABA	γ-aminobutyric acid
GAD1/GAD_{67}	glutamine decarboxylase$_{67}$
GAD2/GAD_{65}	glutamine decarboxylase$_{65}$
GCK	glucokinase
Ghrh	growth hormone-releasing hormone
GLUT2	glucose transporter-2
GLUT3	glucose transporter-3
GPR81/HCAR1	G protein-coupled membrane lactate receptor
IIH	insulin-induced hypoglycemia
INS	insulin
MBH	mediobasal hypothalamus
nNOS/NOS1	neuronal nitric oxide synthase
NO	nitric oxide
OVX	ovariectomy
sc	subcutaneous
SF-1/Nr5a1	steroidogenic factor-1
Slc1A2/GLT-1	vesicular glutamate transporter-1

Supplementary Information

The online version contains supplementary material available at https://doi.org/10.1186/s12868-025-00940-0.

Supplementary Material 1

Supplementary Material 2

Acknowledgements
Not applicable.

Author contributions
S.C.R. conceptualized the research plan; S.C.R., M.B.P., and S.S. carried out the research; S.C.R. prepared all figures; S.C.R. and K.P.B. wrote and edited the main manuscript text.

Funding
This research was supported by NIH grant DK 109382.

Data availability
Data will be provided upon reasonable request to the Corresponding Author.

Declarations

Ethical approval
Studies performed here were approved by the University of Louisiana Monroe Institutional Animal Care and Use Committee, reference no. 19AUG-KPB-01, in accordance with the National Institutes of Health (NIH) Guide for Care and Use of Laboratory Animals, 8th Edition.

Consent for publication
Not applicable.

Competing interests
The authors declare no competing interests.

Received: 17 December 2024 / Accepted: 18 February 2025
Published online: 24 February 2025

References

1. Auer RN. Hypoglycemic brain damage. Forensic Sci Int. 2004;146(2–3):105–10. https://doi.org/10.1016/j.forsciint.2004.08.001.
2. Hamed SA. Brain injury with diabetes mellitus: evidence, mechanisms and treatment implications. Expert Rev Clin Pharmacol. 2017;10(4):409–28. https://doi.org/10.1080/17512433.2017.1293521.
3. Zhao S, Liu Z, Ma L, Yin M, Zhou Y. Potential biomarkers in hypoglycemic brain injury. Forensic Sci Med Pathol. 2023. https://doi.org/10.1007/s12024-023-00681-8.
4. Watts AG, Donovan CM. Sweet talk in the brain: glucosensing, neural networks, and hypoglycemic counterregulation. Front. Neuroendocrinol. 31, 32–43 (2010). doi: 0.1016/j.yfrne.2009.10.006.
5. Sapkota S, Ali MH, Alshamrani AA, Bheemanapally K, Briski KP. Ghrhr neurons from the ventromedial hypothalamic nucleus provide dynamic and sex-specific input to the brain glucose-regulatory network. Neuroscience. 2023;529:73–87. https://doi.org/10.1016/j.neuroscience.2023.08.006.
6. Sapkota S, Roy SC, Shrestha R, Briski KP. Steroidogenic factor-1 regulation of dorsomedial ventromedial hypothalamic nucleus Ghrh neuron transmitter marker and Estrogen receptor gene expression in male rat. ASN Neuro. 2024;15(11):2350–8. https://doi.org/10.1080/17590914.2024.2368382.
7. Roy SC, Sapkota S, Pasula MB, Katakam S, Shrestha R, Briski KP. Differential glucose transporter-2 regulation of dorsomedial versus ventrolateral ventromedial hypothalamic nucleus GABAergic neuron counterregulatory transmitter and energy sensor gene expression. Sci Rep. 2024;14:14220. https://doi.org/10.1038/s41598-024-64708-y.

8. Picón-Pagès P, Buendia-Garcia J, Muñoz FJ. Functions and dysfunctions of nitric oxide in brain. Biochim Biophys Acta Mol Basis Dis. 2019;1865(8):1949–67. https://doi.org/10.1016/j.bbadis.2018.11.007.
9. Fioramonti X, Marsollier N, Song Z, Fakira KA, Patel RM, Brown S, Duparc T, Pica-Mendez A, Sanders NM, Knauf C, Valet P, McCrimmon RJ, Beuve A, Magnan C, Routh VH. Ventromedial hypothalamic nitric oxide production is necessary for hypoglycemia detection and counterregulation. Diabetes. 2010;59(2):519–28. https://doi.org/10.2337/db09-0421.
10. Fioramonti X, Song Z, Vazirani RP, Beuve A, Routh VH. Hypothalamic nitric oxide in hypoglycemia detection and counterregulation: a two-edged sword. Antioxid Redox Signal. 2011;14(3):505–17. https://doi.org/10.1089/ars.2010.3331.
11. Donovan CM, Watts AG. Peripheral and central glucose sensing in hypoglycemic detection. Physiology. 2014;29(5):314–24. https://doi.org/10.1152/physiol.00069.2013.
12. Wood IS, Trayhurn P. Glucose transporters (GLUT and SGLT): expanded families of sugar transport proteins. Brit J Nutr. 2003;89:3–9. https://doi.org/10.1079/BJN2002763.
13. Thorens B, Mueckler M. Glucose transporters in the 21st century. Amer J Physiol Endocrinol Metab. 2010;298:E141–5. https://doi.org/10.1152/ajpendo.00712.2009.
14. Mueckler M, Thorens B. The SLC2 (GLUT) family of membrane transporters. Mol Aspects Med. 2013;34:121–38. https://doi.org/10.1016/j.mam.2012.07.001.
15. Matschinsky FM, Wilson DF. The central role of glucokinase in glucose homeostasis; a perspective 50 years after demonstrating the presence of the enzyme in Islets of Langerhans. Front Physiol. 2019;10:148. https://doi.org/10.3389/fphys.2019.00148.
16. Holman GD. Structure, function, and regulation of mammalian glucose transporters of the SLC2 family. Pflügers Archiv – Eur J Physiol. 2020;472:1155–75. https://doi.org/10.1007/s00424-020-02411-3.
17. Hardie DG, Ross FA, Hawley SA. AMPK: a nutrient and energy sensor that maintains energy homeostasis. Nat Rev Mol Cell Biol. 2012;13:251–62. https://doi.org/10.1038/nrm3311.
18. Hardie DG, Schaffer BE, Brunet A. AMPK: an Energy-Sensing pathway with multiple inputs and outputs. Trends Cell Biol. 2016;26:190–201. https://doi.org/10.1016/j.tcb.2015.10.013.
19. Woods A, Salt I, Scott J, Hardie DG, Carling D. The alpha1 and alpha2 isoforms of the AMP-activated protein kinase have similar activities in rat liver but exhibit differences in substrate specificity in vitro. FEBS Lett. 1996;397:347–51. https://doi.org/10.1016/s0014-5793(96)01209-4.
20. Roy SC, Sapkota S, Pasula MB, Briski KP. *In vivo* Glucose transporter-2 regulation of dorsomedial versus ventrolateral VMN astrocyte metabolic sensor and glycogen metabolic enzyme gene expression. Neurochem. Res. 2024; https://doi.org/10.1007/s11064-024-04246-1
21. Mahmood ASMH, Bheemanapally K, Mandal SK, Ibrahim MMH, Briski KP. Norepinephrine control of ventromedial hypothalamic nucleus glucoregulatory neurotransmitter expression in the female rat: role of monocarboxylate transporter function. Mol Cell Neurosci. 2019;95:51–8. https://doi.org/10.1016/j.mcn.2019.01.004.
22. Bheemanapally K, Alhamyani AR, Ibrahim MMH, Briski KP. Ventromedial hypothalamic nucleus glycogen phosphorylase regulation of metabolic-sensory neuron AMPK and neurotransmitter protein expression: role of L-lactate. Amer J Physiol Regul Integr Comp Physiol. 2021;320:R791–9. https://doi.org/10.1152/ajpregu.00292.2020.
23. Roy SC, Napit PR, Pasula M, Bheemanapally K, Briski KP. G protein-coupled lactate receptor GPR81 control of ventrolateral ventromedial hypothalamic nucleus glucoregulatory neurotransmitter and 5'-AMP-activated protein kinase expression. Amer J Physiol Regul Integr Comp Physiol. 2023;324:R20–34. https://doi.org/10.1152/ajpregu.00100.2022.
24. Napit PR, Ali MH, Shakya M, Mandal SK, Bheemanapally K, Mahmood ASMH, Ibrahim MMH, Briski KP. Hindbrain Estrogen receptor regulation of counter-regulatory hormone secretion and ventromedial hypothalamic nucleus glycogen content and glucoregulatory transmitter signaling in hypoglycemic female rats. Neuroscience. 2019;411:211–21. https://doi.org/10.1016/j.neuroscience.2019.05.007.
25. Briski KP, Mandal SK, Bheemanapally K, Ibrahim MMH. Effects of acute versus recurrent insulin-induced hypoglycemia on ventromedial hypothalamic nucleus metabolic-sensory neuron AMPK activity: impact of alpha1-adrenergic receptor signaling. Brain Res Bull. 2020;157:41–50. https://doi.org/10.1016/j.brainresbull.2020.01.013.
26. Ibrahim MMH, Bheemanapally K, Alhamami HN, Briski KP. Effects of intracerebroventricular glycogen phosphorylase inhibitor CP-316,819 infusion on hypothalamic glycogen content and metabolic neuron AMPK activity and neurotransmitter expression in the male rat. J Mol Neurosci. 2020;70:647–58. https://doi.org/10.1007/s12031-019-01471-0.
27. Bheemanapally K, Ibrahim MMH, Briski KP. Analysis of glycogen regulation of ventromedial hypothalamic nucleus astrocyte and neuron glucogenic amino acid content by combinatory immunocytochemistry / laser-catapult microdissection / UHPLC-electrospray ionization-mass spectrometry. Sci Rep. 2021;11:6079. https://doi.org/10.1038/s41598-021-95646-8.
28. Bheemanapally K, Briski KP. Differential G-protein-coupled Estrogen receptor-1 regulation of counter-regulatory neurotransmitter marker and 5'-AMP-activated protein kinase expression in ventrolateral versus dorsomedial ventromedial hypothalamic nucleus. Neuroendocrinology. 2024;114:25–41. https://doi.org/10.1159/000533627.
29. Ali MH, Alshamrani AA, Napit PR, Briski KP. Single-cell multiplex qPCR evidence for sex-dimorphic glutamate decarboxylase, Estrogen receptor, and 5'-AMP-activated protein kinase alpha subunit mRNA expression by ventromedial hypothalamic nucleus GABAergic neurons. J Chem Neuroanat. 2022;27:102132. 10.1016-/j.jchemneu.2022.102132.
30. Ali MH, Alshamrani AA, Briski KP. Hindbrain lactate regulation of hypoglycemia-associated patterns of catecholamine and metabolic-sensory biomarker gene expression in A2 noradrenergic neurons innervating the ventromedial hypothalamic nucleus in male versus female rat. J Chem Neuroanat. 2022;22:102102. https://doi.org/10.1016/j.jchemneu.2022.102102.
31. Alshamrani AA, Ibrahim MMH, Briski KP. Effects of short-term food deprivation on catecholamine and metabolic-sensory biomarker gene expression in hindbrain A2 noradrenergic neurons projecting to the forebrain rostral preoptic area: impact of negative versus positive estradiol feedback. IBRO Neurosci Rep. 2022;13:38–46. https://doi.org/10.1016/j.ibneur.2022.06.001.
32. Livak KJ, Schmittgen TD. Analysis of relative gene expression data using real-time quantitative PCR and the $2^{-\text{Delta Delta C(t)}}$ method. Methods. 2001;25:402–8. https://doi.org/10.1006/meth.2001.1262.
33. Behar KL. GABA synthesis and metabolism. In: Encyclopedia of Neuroscience, pp. 433–439, 2009. https://doi.org/10.1016/B978-008045046-9.01240-7
34. Martin DL, Barke KE. Are GAD65 and GAD67 associated with specific pools of GABA in brain? Perspect. Develop Neurobiol. 1998;5:119–29.
35. Tavazzani E, Tritto S, Spaiardi P, Botta L, Manca M, Prigoni I, Masetto S, Russo G. Glutamic acid decarboxylase 67 expression by a distinct population of mouse vestibular supporting cells. Front Cell Neurosci. 2014;8:428. https://doi.org/10.3389/fncel.2014.00428.
36. Schousboe A, Waagepetersen HS. Gamma-Aminobutyric Acid (GABA). Refer. Mod. Neurosci. Biobehav. Psychol. 2017. https://doi.org/10.1016/B978-0-12-809324-5.02341-5
37. Tian N, Petersen C, Kash S, Baekkeskov S, Copenhagen D, Nicoll R. The role of the synthetic enzyme GAD65 in the control of neuronal gamma-aminobutyric acid release. Proc. Natl. Acad. Sci. USA. 1999; 96(22): 12911–12916. https://doi.org/10.1073/pnas.96.22.12911
38. Lee SE, Lee Y, Lee GH. The regulation of glutamic acide decarboxylases in GABA neurotransmission in the brain. Arch Pharm Res. 2019;42:1031–9.
39. Chattopadhyaya B, Di Cristo G, Wu CZ, Knott G, Kuhlman S, Fu Y, Palmiter RD, Huang ZJ. GAD67-mediated GABA synthesis and signaling regulate inhibitory synaptic innervation in the visual cortex. Neuron. 2007;54(6):889–903. https://doi.org/10.1016/j.neuron.2007.05.015.
40. Koch U, Magnusson AK. Unconventional GABA release: mechanisms and function. Curr Opin Neurobiol. 2009;19(3):305–10. https://doi.org/10.1016/j.conb.2009.03.006.
41. Chowdhury GMI, Wang P, Ciardi A, Mamillapalli R, Johnson J, Zhu W, Eid T, Behar K, Chan O. Impaired glutamatergic neurotransmission in the ventromedial hypothalamus May contribute to defective counterregulation in recurrently hypoglycemic rats. Diabetes. 2017;66(7):1979–89. https://doi.org/10.2337/db16-1589.
42. Cheung CC, Kurrasch DM, Liang JK, Ingraham HA. Genetic labeling of steroidogenic factor-1 (SF-1) neurons in mice re veals ventromedial nucleus of the hypothalamus (VMH) circuitry beginning at neurogenesis and development of a separate non-SF-1 neuronal cluster in the ventrolateral VMH. J Comp Neural. 2013;521(6):1268–88.
43. Kim DW, Yao Z, Graybuck LT, Kim TK, Nguyen TN, Smith KA, Fong O, Yi L, Koulena N, Pierson N, Shah S, Lo L, Pool AH, Oka Y, Pachter L, Cai L, Tasic B, Zeng H, Anderson DJ. Multimodal analysis of cell types in a hypothalamic node controlling social behavior. Cell. 2019;179:713–28..el 7.

44. Navarro M, Rodriquez de Fonseca F, Alvarez E, Chowen JA, Zueco JA, Gomez R, Eng J, Blázquez E. Colocalization of glucagon-like peptide-1 (GLP-1) receptors, glucose transporter GLUT-2, and glucokinase mRNAs in rat hypothalamic cells: evidence for a role of GLP-1 receptor agonists as an inhibitory signal for food and water intake. J Neurochem. 1996;67(5):1982–91. https://doi.org/10.1046/j.1471-4159.1996.67051982.x.
45. Roncero I, Alvarez E, Vázquez P, Blázquez E. Functional glucokinase isoforms are expressed in rat brain. J Neurochem. 2000;74(5):1848–57. https://doi.org/10.1046/j.1471-4159.2000.0741848.x.

Publisher's note